ARTICLE TYPE www.rsc.org/xxxxxx | XXXXXXXX

To access the final edited and published work see http://dx.doi.org/10.1039/b915169a

Tailored Adsorption of His_6-tagged Protein onto Nickel(II) Cyclam Grafted Mesoporous Silica

Darragh A. Gaffney*[a], Sarah O'Neill[a], Mary O'Loughlin[b], Ulf Hanefeld[c], Jakki Cooney[b], Edmond Magner[a]

Received (in XXX, XXX) Xth XXXXXXXXX 200X, Accepted Xth XXXXXXXXX 200X
First published on the web Xth XXXXXXXXX 200X
DOI: 10.1039/b000000x

The specific immobilisation of a histidine tagged protein, Spi, onto mono-anchored nickel(II) cyclam functionalised SBA-15 is reported.

Enzymes have the capacity to catalyse reactions with high regio- and chemoselectivity while operating under mild conditions, properties which have led to a surge in the use of biocatalysts. However, the application of biocatalsyts in many industrial applications is restricted as the process of removing the enzyme from the reaction mixture can cause denaturation of the biocatalyst. Immobilized enzymes can display activities superior to that of the free enzyme[1-4] while remaining stable and exhibiting significant catalytic activity in harsh media such as non-aqueous solvents[5, 6]. However, more often than not immobilized enzymes display activities significantly less than free enzyme[7]. Mesoporous silicates (MPS) have been extensively studied as supports for enzymes[8]. Some of the properties which make MPS attractive as solid supports include narrow pore size distributions, large surface areas (up to 1500 m^2/g), chemical and thermal stability, the ability to chemically functionalise the surface, and pore dimensions capable of accommodating enzymes. While a wide range of proteins have been immobilised on to MPS[9, 10] in many cases the immobilised enzyme displays reduced activity in comparison to the free enzyme and can not be efficiently recycled due to leaching of the enzyme from the support.

Mesoporous organic-inorganic hybrid materials[11-14] possess co-ordination binding sites and hydrophobic/hydrophilic binding patches. Among the possibilities offered by this class of solids is the ability to strongly chelate metal cations which can remain chemically accessible. Previous reports of silicates functionalised with cationic metals have been used for electroconductive[15], biocatalytic[16,17] and optical applications[18]. Tailoring the surface of a mesoporous silicate and the surface of a protein can enable specific anchoring of the protein. This can negate consideration of the many variables involved when immobilising a protein onto MPS[19]. The approach taken here utilises a technique in widespread use in recombinant protein purification; immobilised metal affinity chromatography (IMAC). Adsorption of histidine-tagged proteins on to Ni or Co functionalised surfaces has been demonstrated previously[3,16,20],Here we present a method for the generation of a supported biocatalyst in which SBA-15 is functionalised with Ni^{2+} and used as a host material for the specific adsorption of a model protein, His_6-tagged Spi.

SBA-15 is a mesoporous silicate generated from a non-ionic surfactant template and displays a hexagonally ordered array of mesopores with microporous interconnections, resulting in a unique 3-D micro-mesoporous network. Cyclam (1,4,8,11-tetraazacyclotetradecane) can bind to a range of transition metals, including nickel. Ni-cyclam complexes have been extensively studied[21], in particular the tetra-*N*-substituted complexes[22, 23]. Cyclam which is mono-tethered to the surface of SBA-15 displays a greater degree of metal uptake than di- or tetra-tethered cyclams[24]. In this study, a mono-*N*-substituted Ni^{2+} cyclam complex was attached to the surface of a mesoporous silicate in a stepwise manner (Scheme 1). The protein used as a model system, Spi[25], is a small protease inhibitor from the human pathogen *Streptococcus pyogenes*. The His_6-tagged form was chosen due to its small size (14.7 kDa) and favorable pI (5.4). Spi does not possess a high surface charge, ensuring that electrostatic interactions with the carrier will be minimized.

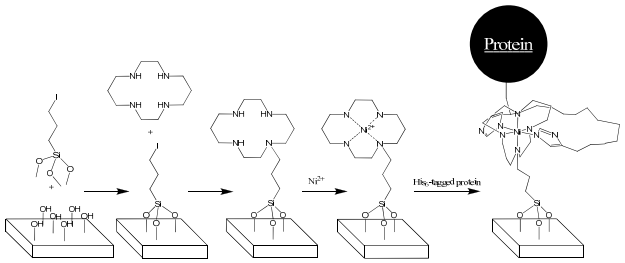

Scheme 1. Surface modification of SBA-15 with Ni-cyclam and subsequent attachment of a His_6-tagged protein

SBA-15-Ni-cyclam† was prepared[26] from SBA-15 with a pore diameter of 8.5 nm. SBA-15 was functionalised with 3-iodo-trimethoxypropylsilane to provide an iodo-functionality on the silicate surface. The iodo-functionality was required for the attachment of 1,4,8,11-tetraazacyclotetradecane (cyclam) onto the surface. Unfunctionalised SBA-15 was used as the control material. The synthesis can be monitored from the colour changes which occur, depending on the functional groups present. The silicate itself is a white powder and upon attachment of the iodo functionality it turned a green colour. This green colour faded as the iodo functionality was removed and attachment of the cyclam occurred, yielding a white powder once again. Upon complexation of nickel with the cyclam ring the final material remained a pale yellow colour indicating that nickel cyclam had been formed[27]. SBA-15 showed a pore diameter of 8.5 nm, estimated from condensation relative pressure[28], and a BET surface area of 742 m^2/g (Table 1). Low-angle XRD analysis displayed a very

Table 1 Physicochemical properties obtained from nitrogen adsorption analysis for the mesoporous materials used in this study.

	BET Surface Area (m^2/g)	Pore Volume (cm^3/g)	Pore Diameter (nm)[a]
SBA-15	742	0.9	8.5
SBA-15-Ni-cyclam	138	0.13	5.5

[a] estimated from condensation relative pressure[28]

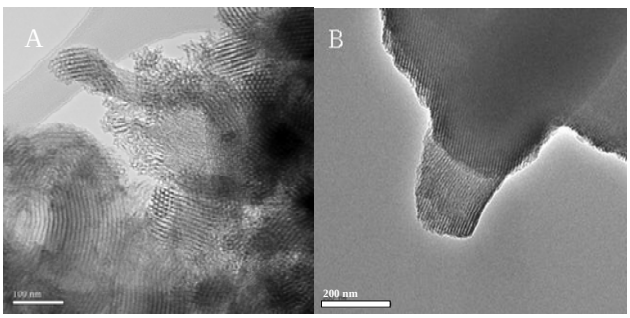

Fig. 1 TEM micrographs of (A) SBA-15 and (B) SBA-15-Ni-cyclam showing the order and structure of the silicate scaffold have been retained.

intense diffraction peak and two weaker peaks, assigned to the 100, 110 and 200 planes respectively, which are characteristic of the material[29]. The procedure required for the surface functionalisation of the silicate had a notable effect on the original substrate structure, in particular the surface area, pore volume and pore diameter. This was evident from the reduced N_2 adsorption capacity after functionalisation. SBA-15-Ni-cyclam displayed a greater than 80% reduction in surface area (138 m^2/g) and a pore diameter of 5.5 nm. XPS analysis of SBA-15-cyclam confirmed the presence of nitrogen with a binding energy consistent with carbon binding. The presence of residul unreacted iodine in an alkyl environment was also detected in this sample. Analysis of SBA-15-Ni-cyclam displayed a similar spectrum to SBA-15-cyclam, with the addition of a peak corresponding to nickel in a nitrogen-organic environment[30]. While TEM images of SBA-15-Ni-cyclam (Figure 1) display the hexagonal structure of the parent SBA-15 material, XRD analysis of SBA-15-Ni-cyclam displayed a loss of diffraction peaks for the 110 and 200 planes as well as the prominent 100 plane. This data is consistent with reduced scattering contrast between the silica wall and the pore network due to functionalisation[28] as well as a possible partial collapse of the pore wall structure. To determine whether the change in N_2 adsorption capacity was due to the reaction conditions or the metal functionalisation, SBA-15 was exposed to the functionalisation conditions without reagents. N_2 adsorption analysis displayed a smaller reduction in BET surface area (368 m^2/g) and an increase in pore diameter (9.4 nm) indicating that the changes in pore diameter and surface area of SBA-15-Ni-cyclam are a consequence of the incorporation of the large organic macrocycle into the pore channel[27] coupled with a partial collapse of the pore structure. Elemental analysis of SBA-15-cyclam showed no presence of nickel as expected whereas SBA-15-Ni-cyclam contained 1.18% w/w nickel (201 µmole g^{-1}). SBA-15-Ni-cyclam had a N/Ni molar ratio of 6:1, close to the 4:1 ratio expected for complete nickel-cyclam coordination. A nickel/protein excess ensures availability of the metal for protein binding as well as compensating for the presence of micropores in the SBA-15 scaffold which are inaccessible to the protein. Thermal gravimetric analysis of SBA-15, SBA-15-cyclam and SBA-15-Ni-cyclam, displayed a sharp weight loss at 50ºC, corresponding to the evaporation of physisorbed water. Above 50ºC, the as-synthesised SBA-15 did not display any further significant reduction in weight,as expected. However, SBA-15-cyclam and SBA-15-Ni-cyclam both display weight losses from 300 – 400 ºC with SBA-15-Ni-cyclam displaying a markedly greater loss than SBA-15-cyclam (29 and 17% respectively). These weight losses can be attributed to the loss of Ni-cyclam and cyclam, respectively.

The functionalised silicate, SBA-15-Ni-cyclam and the unfunctionalised silicate, SBA-15 were examined for specific adsorption of His_6-Spi. The dimensions of His_6-Spi were calculated to be 3.7 x 3.3 x 2.4 nm[29]. SBA-15-Ni-cyclam has a pore of 5.5 nm, large enough to accommodate the protein. SBA-15 and SBA-15-Ni-cyclam were incubated in a solution of the protein in 25 mM TRIS buffer pH 7.4. Performing the immobilisation at neutral pH ensures that the surface of His_6-Spi (pI 5.4) and SBA-15 (pI 3.9) both possess an overall negative charge, conditions which should prevent favourable electrostatic interactions between the protein and the silicate as well as directing interactions through the His_6-tag and the nickel on the silicate surface. However, when both SBA-15 and SBA-15-Ni-cyclam were incubated with the protein solution, they displayed close to complete uptake of the His_6-Spi, with SBA-15 and SBA-15-Ni-cyclam adsorbing 7.2 µmole g^{-1} (91% of protein) and 6.7 µmole g^{-1} (85% of protein), respectively (Table 2).

To optimise the interaction and increase the binding specificity between Ni^{2+} and His_6-tag, pH was adjusted to 9, increasing the overall surface charges of the silicate and the protein. The incubation was also performed at varying ionic strenghts, 50 mM, 500 mM and 1 M. At low ionic strength (50 mM), there was approximatley 50% reduction in protein uptake onto SBA-15 and SBA-15-Ni-cyclam (3.76 µmole g^{-1} for both silicates). As the ionic strength increased, the amount of protein adsorbed increased correspondingly, to ~5.35 µmole g^{-1} (SBA-15 and SBA-15-Ni-cyclam) on incubation at 500 mM and 6.45 and 6 µmole g^{-1} at an ionic strength of 1 M. In determining the type of interaction between protein and silicate (ionic, hydrophobic, nickel coordination) the adsorption behaviour observed indicated that the interaction between protein and support was not electrostatic. Such interactions between protein and support would have resulted in a reduction of protein uptake as the ionic strength increased, due to the shielding effect of the increased ion content on both the protein and silicate surfaces. However, the opposite occurred, indicating that adsorption was likely to be occurring either through hydrophobic interactions or nickel coordination. As adsorption occurred on both nickel functionalised material and the unfunctionalised material on exposure to high ionic strength, it is reasonable to conclude that adsorption is occurring through the hydrophobic patches on the Spi surface and not through nickel co-ordination as desired. PEG_{400} (2%v/v) was added, essentially abolishing

Table 2 Summary of incubation conditions and protein amounts adsorbed onto silicate supports.

Protein (pH, Ionic strength and PEG_{400} content	*Concentration (*μM*)*	*SBA-15 (*μmole g^{-1}*)*	*SBA-15-Ni-cyclam (*μmole g^{-1}*)*
His_6-Spi (pH 7, 25 mM, 0%)	39.3	7.2	6.7
His_6-Spi (pH 9, 50 mM, 0%)	36	3.76	3.76
His_6-Spi (pH 9, 500 mM, 0%)	36	5.35	5.29
His_6-Spi (pH 9, 1 M, 0%)	36	6.45	6
His_6-Spi (pH 7.4, 100 mM, 2%)	17.4	0.13	2.73
Spi (pH 7.4, 25 mM, 2%)	37.1	0	0.43

non-specific binding of His_6-Spi to unfunctionalised SBA-15. After pre-incubation of His_6-Spi in 2% PEG_{400}, SBA-15-Ni-cyclam displayed a protein uptake of 2.73 μmole g^{-1} (79% of protein), whereas the unfunctionalised SBA-15 displayed a protein uptake of only 0.13 μmole g^{-1} (4%). Specific binding of His_6-Spi to SBA-15-Ni-cyclam in the presence of PEG is lower due to the lower initial concentration of protein (17.4 vs. 39.3 μM). Leaching studies of His_6-Spi immobilised onto SBA-15-Ni-cyclam displayed no desorption of the protein. To further confirm the specific nature of the interaction of the histidine tag and the Ni(II)-cyclam complex, SBA-15 and SBA-15-Ni-cyclam were exposed to Spi from which the His_6-tag had been removed by proteolysis. SBA-15 displayed no protein uptake and SBA-15-Ni-cyclam displayed a negligible uptake of 0.43 μmole g^{-1} (7%). This result provides strong evidence that the interaction between His_6-Spi and SBA-15-Ni-cyclam in the presence of 2% PEG_{400} is as a result of coordination of the Ni^{2+} by the imidazole rings of the His_6-tag.

As protein uptake occurred primarily on the nickel functionalised material, we conclude that adsorption occurred through the His_6-tag on available nickel sites. These results open up the possibility of immobilising any His_6-tagged protein/enzyme for use as a stable and reusable biocatalyst as well as obviating the necessity of an often laborious search for ideal immobilisation conditions for specific proteins/enzymes.

Notes and references

[a]*Materials and Surface Science Institute,SFI-SRC in Solar Energy Conversion, Department of Chemical and Environmental Science, University of Limerick, Limerick, Ireland. Tel: +353-61-202629 Email: Edmond.Magner@ul.ie*

[b]*Materials and Surface Science Institute, Department of Life Sciences, University of Limerick, Limerick, Ireland. Tel: +353-61-202880 Email: Jakki.Cooney@ul.ie*

[c]*Gebouw voor Scheikunde, Afdeling Biotechnologie, Julianalaan 136, 2628 BL Delft, The Netherlands. Tel: +31-15-2789304 Email: U.Hanefeld@tudelft.nl*

†Electronic Supplementary Information (ESI) available: [Synthesis of SBA-15-Ni-cyclam, Synthesis of His_6-Spi and Spi, Enzyme adsorption procedure, Leaching experiments, Characterization data; Nitrogen adsorption analysis, Low-angle XRD, XPS]. See DOI: 10.1039/b000000x/

The assistance of Dr Fathima Laffir (XPS) and of Dr. Sarah Hudson for general discussions are gratefully acknowledged. This work was funded by Science Foundation Ireland (RFP06/CHP001).

1 U. Hanefeld, L. Gardossi, and E. Magner, *Chemical Society Review*, 2009, **38**, 453.

2 J. Deere, E. Magner, J. G. Wall, and B. K. Hodnett, *Chemical Communications*, 2001, **5**, 465-466.

3 M. Miyazaki, J. Kaneno, S. Yamaori, T. Honda, M. P. P. Briones, M. Uehara, K. Arima, K. Kanno, K. Yamashita, Y. Yamaguchi, H. Nakamura, H. Yonezawa, M. Fujii, and H. Maeda, *Protein & Peptide Letters*, 2005, **12**, 207-210.

4 W. Tischer and V. Kasche, *Trends in Biotechnology*, 1999, **17**, 326-335.

5 A. M. Klibanov, *Nature*, 2001, **409**, 241-246.

6 M. Petkar, A. Lali, P. Caimi, and M. Daminati, *J. of Mol. Catal. B: Enzymatic*, 2006, **39**, 83-90.

7 J. Aburto, M. Ayala, I. Bustos-Jaimes, C. Montiel, E. Terres, J. M. Dominguez, and E. Torres, *Microporous and Mesoporous Materials*, 2005, **83**, 193-200.

8 Y. Wan and D. Y. Zhao, *Chem. Rev.*, 2007, **107**, 2821-2860.

9 M. Hartmann, *Chem. Mater.*, 2005, **17**, 4577-4593.

10 H. H. P. Yiu and P. A. Wright, *J. Mater. Chem*, 2005, **15**, 3690-3700.

11 A. Sayari and M. Jaroniec, eds., *Recent developments in the synthesis and chemistry of periodic mesoporous organosilicas*, Elsevier, 2002.

12 S. Guan, S. Inagaki, T. Ohsuna, and O. Terasaki, *Microporous and Mesoporous Materials*, 2001, **44-45**, 165-172.

13 K. Tsuji, C. W. Jones, and M. E. Davis, *Microporous and Mesoporous Materials*, 1997, **29**, 339-349.

14 C. P. Jaroniec, M. Kruk, M. Jaroniec, and A. Sayari, *J. Phys. Chem. B*, 1998, **102**, 5503-5510.

15 J. F. Diaz, K. J. Balkus, F. Bedioui, V. Kurshev, and L. Kevan, *Chemistry of Materials*, 1997, **9**, 61-67.

16 K. E. Cassimjee, T. Martin, B. Cecilia, and B. Per, *Biotechnology and Bioengineering*, 2008, **99**, 712-716.

17 Y. S. Cho, J. C. Park, B. Lee, Y. Kim, and J. Yi, *Catalysis Letters*, 2002, **81**, 89-96.

18 R. J. P. Corriu, A. Mehdi, C. Reye, and C. Thieuleux, *Chemical Communications*, 2003, 1564-1565.

19 S. Hudson, J. Cooney, and E. Magner, *Angewandte Chemie International Edition*, 2008, **47**, 8582-8594.

20 E. Kang, J.-W. Park, S. J. McClellan, J.-M. Kim, D. P. Holland, G. U. Lee, E. I. Franses, K. Park, and D. H. Thompson, *Langmuir*, 2007, **23**, 6281-6288.

21 T. H. Kaden, *Helvetica Chimica Acta*, 1970, **53**, 617-622.

22 M. Meyer, V. Dahaoui-Gindrey, C. Lecomte, and R. Guilard, *Coordination Chemistry Reviews*, 1998, **178-180**, 1313-1405.

23 C. Bucher, E. Duval, J.-M. Barbe, J.-N. Verpeaux, C. Amatore, R. Guilard, L. Le Pape, J.-M. Latour, S. Dahaoui, and C. Lecomte, *Inorganic Chemistry*, 2001, **40**, 5722-5726.

24 M. Etienne, Stephanie Goubert-Renaudin, Yoann Rousselin, Claire Marichal, Franck Denat, Bendicte Lebeau, and A. Walcarius, *Langmuir*, 2009, **25**, 3137-3145.

25 T. F. Kagawa, P. W. O'Toole, and J. C. Cooney, *Molecular Microbiology*, 2005, **57**, 650-666.

26 G. Dubois, Robert J. P. Corriu, Catherine Reyé, Stéphane Brandès, Franck Denat, and R. Guilard, *Chemical Communications*, 1999, 2283.

27 J. Lalitham and V. R. Vijayaraghavan, *Proceedings Indian Academy of Science (Chem. Sci.)*, 2000, **112**, 507-514.

28 M. Kruk and M. Jaroniec, *Chemistry of Materials*, 2001, **13**, 3169-3183.

29 D. Zhao, Q. Huo, J. Feng, B. F. Chmelka, and G. D. Stucky, *J. Am. Chem. Soc.*, 1998, **120**, 6024-6036.

30 NIST X-ray Photoelectron Spectroscopy Database, Version 3.5, National Institute of Standards and Technology, Gaithersburg, 2003.